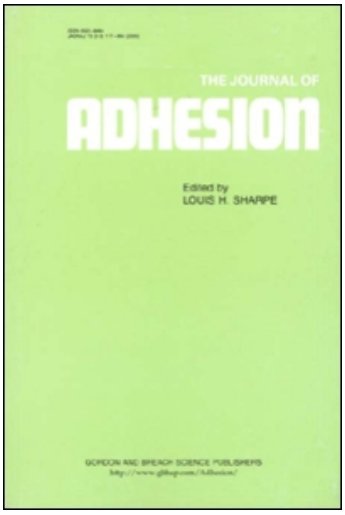

The Journal of Adhesion
Publication details, including instructions for authors and subscription information:
http://www.informaworld.com/smpp/title~content=t713453635

Adhesion-Delamination Mechanics of a Prestressed Circular Film Adhered onto a Rigid Substrate

Ming-fung Wong[a]; Gang Duan[a]; Kai-tak Wan[b]
[a] Mechanical Engineering, University of Missouri-Rolla, Rolla, Missouri, USA [b] Mechanical Engineering, Biological and Chemical Engineering, University of Missouri-Rolla, Rolla, Missouri, USA

To cite this Article Wong, Ming-fung , Duan, Gang and Wan, Kai-tak(2007) 'Adhesion-Delamination Mechanics of a Prestressed Circular Film Adhered onto a Rigid Substrate', The Journal of Adhesion, 83: 1, 67 — 83
To link to this Article: DOI: 10.1080/00218460601102878
URL: http://dx.doi.org/10.1080/00218460601102878

The Journal of Adhesion, 83:67–83, 2007

ISSN: 0021-8464 print/1545-5823 online
DOI: 10.1080/00218460601102878

Taylor & Francis
Taylor & Francis Group

Adhesion–Delamination Mechanics of a Prestressed Circular Film Adhered onto a Rigid Substrate

Ming-fung Wong
Gang Duan
Mechanical Engineering, University of Missouri–Rolla, Rolla, Missouri, USA

Kai-tak Wan
Mechanical Engineering, Biological and Chemical Engineering, University of Missouri–Rolla, Rolla, Missouri, USA

A thin circular film clamped at the periphery is adhered to the planar surface of a rigid cylindrical punch. An external tensile load is applied to the punch, causing the film to delaminate from the substrate and the circular contact edge to contract. The film spontaneously separates from the punch, or pulls off, when the contact radius reduces to a range between 0.1758 and 0.3651 of the film radius, depending on the magnitude of the residual membrane stress. The mechanical delamination process is derived by a thermodynamic energy balance based on a coupled interfacial adhesion and residual membrane stress. The theoretical model has significant implications in nanoforce measurement, microelectromechanical systems (MEMS) comprising active moveable films, and biological cell adhesion.

Keywords: Adhesion; Delamination; Pull in; Pull off; Residual stress; Thin film

1. INTRODUCTION

As nanotechnology advances, thin film adhesion and delamination become important issues in many respects, especially in electronic devices and biological phenomena. In many microelectromechanical systems (MEMS) such as micropumps [1–3], microvalves [4], microactuators [5,6], and radio frequency (RF) switches [7–11], undesirable

Presented in part at the 29th Annual Meeting of the Adhesion Society, Inc., Jacksonville, Florida, USA, 19–22 February 2006.

Address correspondence to Kai-tak Wan, Mechanical and Aerospace Engineering, University of Missouri–Rolla, ME205, 1870 Miner Circle, Rolla, MO 65409-0050, USA. E-mail: wankt@umr.edu

intersurface forces (*e.g.*, electrostatics due to stray charges, meniscus formation due to water condensation, van der Waals interactions, and Derjaguin-Landau-Verwey-Overbeek (DLVO) double layers [12,13]) can lead to stiction of moveable films, which in turn causes severe malfunction and limited reliability and life span. Residual membrane stresses induced in the films as a result of fabrication processes, mismatch of thermal expansion coefficients of film and substrate, and heat dissipation during device operation further complicate the stiction problems. To improve the design criteria and to assess component reliability, a better understanding of the device behavior due to the coupled stiction and residual stresses is indispensable. In biology, individual cells stick together *via* nonspecific (*e.g.*, electrostatic) and specific (*e.g.*, ligand–receptor interactions) to form multicell aggregates, two- and three-dimensional tissues [14]. Because most cells are thin-walled capsules with an ultrathin lipid bilayer membrane down to 100 Å in thickness, interactions between cells are achieved by thin film adhesion. There are situations when biochemical processes, osmosis [15,16] and shear due to fluid flow [17,18] generate tensile residual stresses in the cell membranes that are capable of detaching a cell from an adhering substrate. Interfacial adhesion–delamination also provides the key to cell locomotion [14].

Adhesion between solid bodies has been investigated extensively since the development of the successful Johnson–Kendall–Roberts (JKR) and Derjaguin–Muller–Toporov (DMT) models [19,20]. However, these earlier models do not apply to thin films, because the plate-bending and membrane-stretching deformation modes are vastly different from Hertz's contact problem where compressive stress is the governing mode. We have earlier devised a "punch" test where a circular membrane clamped at its perimeter is adhered to a rigid cylindrical punch [21–23] (Figure 1a). As the punch is pulled away by an external tensile load, the contact circle contracts and vanishes at a critical load and punch displacement. A theoretical model was derived and experimentally verified for the interfacial delamination process with a film undergoing mixed bending and stretching deformation and zero residual stress. Wan and Kogut [24] further derived an elastic model for a flexible stretching membrane with zero flexural rigidity and, therefore, no bending moment. A range of residual membrane stresses was considered. In this article, the film is treated as a thin plate undergoing bending in the presence of coupled residual stress and interfacial adhesion, ignoring membrane stretching due to profile change. The model is relevant to a number of MEMS devices and cell membranes.

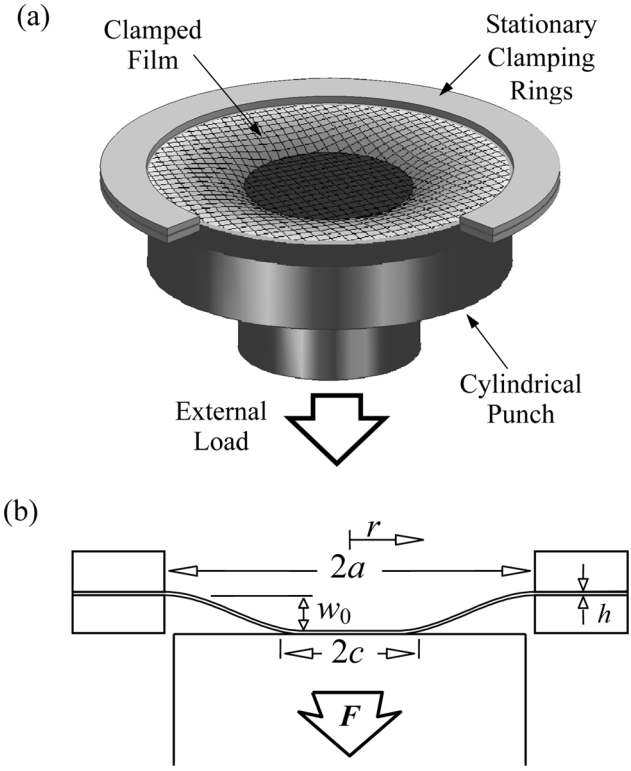

FIGURE 1 (a) Sketch of a clamped circular film adhered to the planar surface of a rigid cylindrical punch. An external tensile load is applied to the punch to drive a delamination along the film–substrate interface. (b) Cross-section of the film–punch system showing the measurable quantities.

2. THEORY

Figure 1a shows a circular film with a radius a, thickness h, elastic modulus E, Poisson's ratio υ, bending rigidity $\kappa = Eh^3/12(1-\upsilon^2)$, and tensile residual stress σ_0 clamped at the perimeter. The film is brought into adhesive contact with the planar surface of a rigid cylindrical punch of radius slightly smaller than a. The film–punch interface has an adhesion energy γ, and the initial contact radius is a. An external tensile force F is applied to the punch so that the film is deformed to a profile, $w(r)$, by plate-bending (Figure 1b). At a critical load and punch displacement, delamination is driven into the film–substrate interface, and the contact radius contracts to c ($<a$).

The force–displacement relation *without* delamination is derived next before incorporating the delamination mechanics.

2.1. Force–Displacement Relation without Delamination

Figure 1 shows the film–punch configuration. The deformation profile of the freestanding annulus ($c \le r \le a$) around the contact circle $w(r)$ is governed by the von Karman equation [21],

$$\underbrace{\kappa\,\nabla^4 w}_{\text{Plate bending}} - \underbrace{\sigma h\,\nabla^2 w}_{\text{Membrane stretching}} = \underbrace{F\,\delta(r)}_{\text{Central external load}}, \tag{1}$$

where ∇^2 is the Laplacian operator in cylindrical coordinates, $\delta(r)$ is the Dirac delta function denoting the applied load acting at the contact edge, and σ is the total membrane stress on the film. Here $\delta(r)$ does not lead to a mathematical singularity because the contact radius never approaches zero (see Appendix 1). Despite a small increase in membrane stress due to profile deformation, the residual membrane stress is assumed to be the only dominant stretching mode, *i.e.*, $\sigma \approx \sigma_0$. For simplicity, normalized parameters as listed in Appendix 2 are used hereafter. Our previous calculation shows the profile to be [21]

$$\omega = \frac{\varphi}{\beta}\left\{C_1[1 - I_0(\beta\xi)] - C_2 K_0(\beta\xi) + C_3 - \frac{\log \xi}{\beta}\right\} \quad \text{for } \zeta \le \xi \le 1, \tag{2}$$

where I_n and K_n are the nth modified Bessel functions of the first and second kind, respectively, and C_1, C_2, and C_3 are constants satisfying the boundary conditions (i) $(\partial\omega/\partial\xi) = 0$ and $\omega = 0$ at $\xi = 1$ at the film perimeter and (ii) $(\partial\omega/\partial\xi) = 0$ at $\xi = \zeta$ at the contact edge, which are found to be

$$C_1 = \frac{1}{\beta^2\zeta}\left[\frac{K_1(\beta) - \zeta K_1(\beta\zeta)}{I_1(\beta)K_1(\beta\zeta) - I_1(\beta\zeta)K_1(\beta)}\right] \tag{2a}$$

$$C_2 = \frac{1}{\beta^2\zeta}\left[\frac{I_1(\beta) - \zeta I_1(\beta\zeta)}{I_1(\beta)K_1(\beta\zeta) - I_1(\beta\zeta)K_1(\beta)}\right] \tag{2b}$$

$$C_3 = \frac{1}{\beta^2\zeta}\left\{\frac{[I_0(\beta) - 1][K_1(\beta) - \zeta K_1(\beta\zeta)] + K_0(\beta)[I_1(\beta) - \zeta I_1(\beta\zeta)]}{I_1(\beta)K_1(\beta\zeta) - I_1(\beta\zeta)K_1(\beta)}\right\}. \tag{2c}$$

The vertical displacement of the punch (*i.e.*, central deflection of the film) is given by

$$\omega_0 = \omega|_{\xi=\zeta} = \frac{\varphi}{\beta}\left\{C_1[1 - I_0(\beta\zeta)] - C_2 K_0(\beta\zeta) + C_3 - \frac{\log \zeta}{\beta}\right\}. \tag{3}$$

Note that the relation $F(w_0)$ or $\varphi(\omega_0)$ is *linear* (*i.e.*, $\varphi \propto \omega_0$), because the curly bracket in Eq. (3) is a constant depending only on the residual stress and the contact radius. This proportionality constant increases for a larger residual stress, leading to a stiffer film and a higher apparent elastic modulus. Similarly, a large punch gives rise to a narrower freestanding annulus and thus a less compliant system with a lower ω_0.

2.2. Thermodynamic Energy Balance for Delamination Mechanics

Once the applied tensile load exceeds a critical threshold, delamination drives into the film–substrate interface. The delamination mechanics is derived by a thermodynamic energy balance. Total energy of the punch–film system is given by

$$U_{\mathrm{T}} = U_{\mathrm{P}} + U_{\mathrm{E}} + U_{\mathrm{S}}. \tag{4}$$

The potential energy U_{P} due to the external load (*i.e.*, energy input) is given by

$$U_{\mathrm{P}} = Fw_0 \qquad \text{or} \qquad \Sigma_{\mathrm{P}} = \varphi\,\omega_0. \tag{4a}$$

The elastic energy stored in the overhanging annulus U_{E} is given by

$$U_{\mathrm{E}} = -\int F\,dw_0 = -\frac{1}{2}Fw_0 \qquad \text{or} \qquad \Sigma_{\mathrm{E}} = -\frac{1}{2}\varphi\,\omega_0. \tag{4b}$$

The integration is obvious because of the *linear* relation $F \propto w_0$ and $\varphi \propto \omega_0$. The energy due to the creation of new surfaces U_{S} is given by

$$U_{\mathrm{S}} = -\pi c^2\gamma \qquad \text{or} \qquad \Sigma_{\mathrm{S}} = -\zeta^2\Gamma. \tag{4c}$$

Substituting Eqs. (4a–c) into Eq. (4), we get

$$U_{\mathrm{T}} = \frac{1}{2}Fw_0 - \pi c^2\gamma \qquad \text{or} \qquad \Sigma_{\mathrm{T}} = \frac{1}{2}\varphi\omega_0 - \zeta^2\Gamma. \tag{5}$$

Coupling of interfacial adhesion and residual stress is obvious when substituting Eq. (3) into Eq. (5). To demonstrate how Eq. (5) accounts for the thin film delamination, we take $\Gamma = 1.00$ and $\beta = 1.00$. Figure 2 shows a family of $\Sigma_{\mathrm{T}}(\zeta)$ for a range of ω_0. For a punch being raised from $\omega_0 = 0$ to 0.05, $\Sigma_{\mathrm{T}}(\zeta)$ possesses one minimum or stable equilibrium at A with $\zeta_{\mathrm{A}} = 0.5702$ and a maximum or unstable equilibrium at a smaller ζ. Further increase in punch displacement to B with $(\omega_0)_{\mathrm{B}} = 0.075$ causes $\Sigma_{\mathrm{T}}(\zeta)$ minimum to shift to $\zeta_{\mathrm{B}} = 0.4464$. Ultimately, when ω_0 reaches 0.1108, the two extrema merge to an inflexion at C with

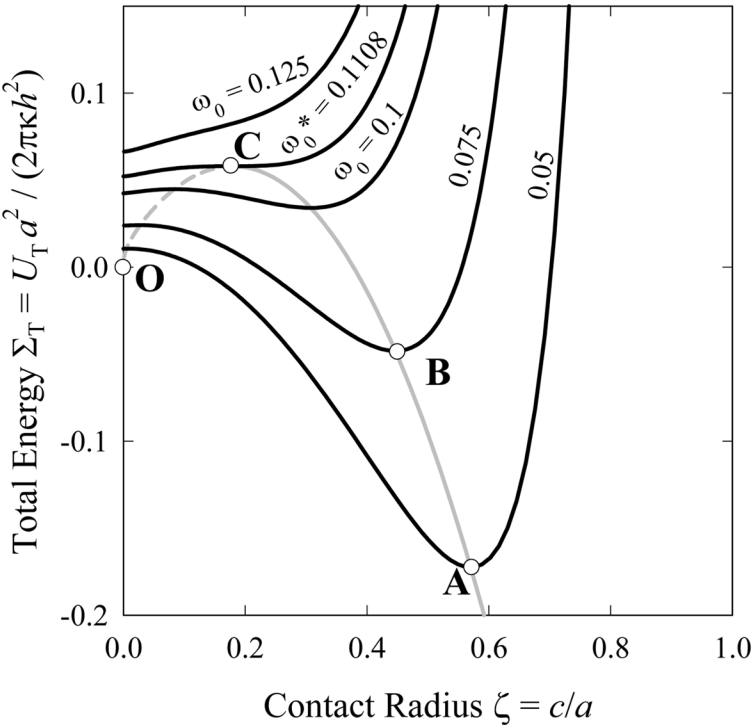

FIGURE 2 Total energy Σ_T of the film–punch system as a function of contact radius and a range of punch displacement for adhesion energy $\Gamma = 1$ (or $\gamma = 2\kappa h^2/a^4$) and residual membrane stress $\beta^2 = 1$ (or $\sigma_0 = \kappa/a^2 h$). The gray curve shows the stable delamination path, and the dashed curve is physically inaccessible. Pull-off occurs at C.

$(d^2\Sigma_T/d\zeta^2) = 0$, $\omega_0^* = 0.1108$, $\zeta^* = 0.1796$, and $\varphi^* = 1.6286$, resulting in a neutral equilibrium. Incremental increase from $\omega_0{}^*$ leads to a spontaneous pull-off, the contact radius drops to zero ($\zeta = 0$), and the film snaps from the substrate. The gray curve ABC joining the minima of $\Sigma_T(\zeta)$ denotes the stable delamination trajectory, whereas the dashed curve OC joining the maxima of $\Sigma_T(\zeta)$ is physically inaccessible and will be ignored.

The situation with a constant β with a varying Γ is considered, followed by a constant Γ with a varying β. Figure 3 shows the stable trajectory of $\Sigma_T(\zeta)$ for $\beta = 1$ and a range of Γ. Each curve exercises a maximum corresponding to pull-off at $\zeta^* = 0.1796$, and the branch with $\zeta < \zeta^*$ is physically inaccessible. The Γ-independency of ζ^* is mathematically verified in the next section. Next, we take $\Gamma = 1$ with

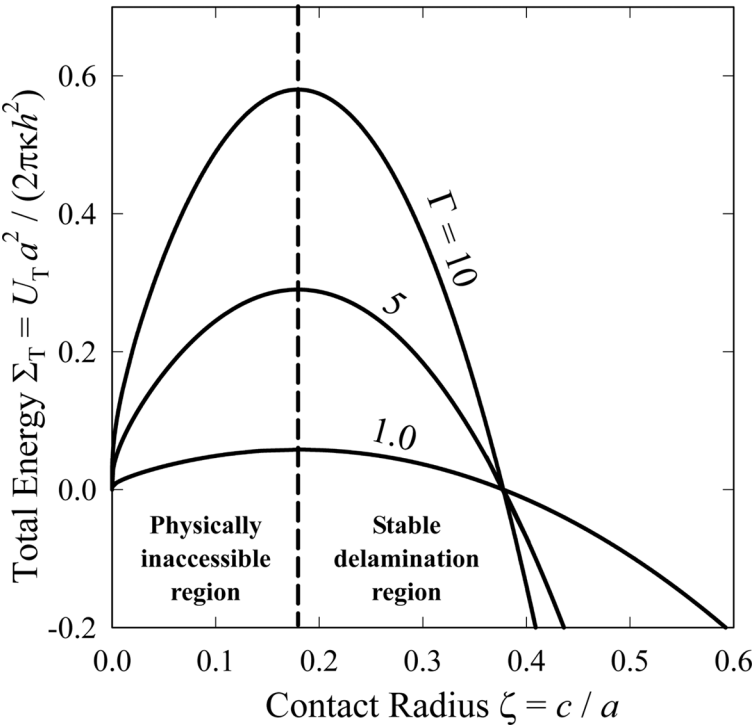

FIGURE 3 For a fixed residual membrane stress ($\beta^2 = 1$), the delamination path for a range of adhesion energy is shown as a function of contact radius. Maximum of each curve corresponds to the pull-off event. The line $\zeta = \zeta^*$ separates the physically inaccessible region from the stable delamination.

a varying β. Figure 4a shows the stable delamination paths and pull-off at the maxima. As the residual stress increases, membrane stretching dominates and bending becomes negligible. Consequently, the pull-off shifts to a smaller punch displacement but a larger contact circle. The pull-off locus follows the gray curve bounded by $\zeta^*_{\min} \le \zeta^* \le \zeta^*_{\max}$ with $\zeta^*_{\min} = 0.1758$ for $\beta = 0$ and $\zeta^*_{\max} = e^{-1} = 0.3679$ for $\beta \to \infty$. A large residual leads to a stiff film where stretching deformation dominates and bending becomes negligible. Figure 4b shows $\zeta^*(\beta^2)$, which is independent of Γ. The open circle on the curve denotes the pull-off event at point C in Figure 2 with $\Gamma = 1.00$ and $\beta = 1.00$.

2.3. Delamination Trajectory

The mechanical delamination response, $F(w_0,c)$ or $\varphi(\omega_0, \zeta)$, of the clamped plate can be derived analytically based on the aforementioned

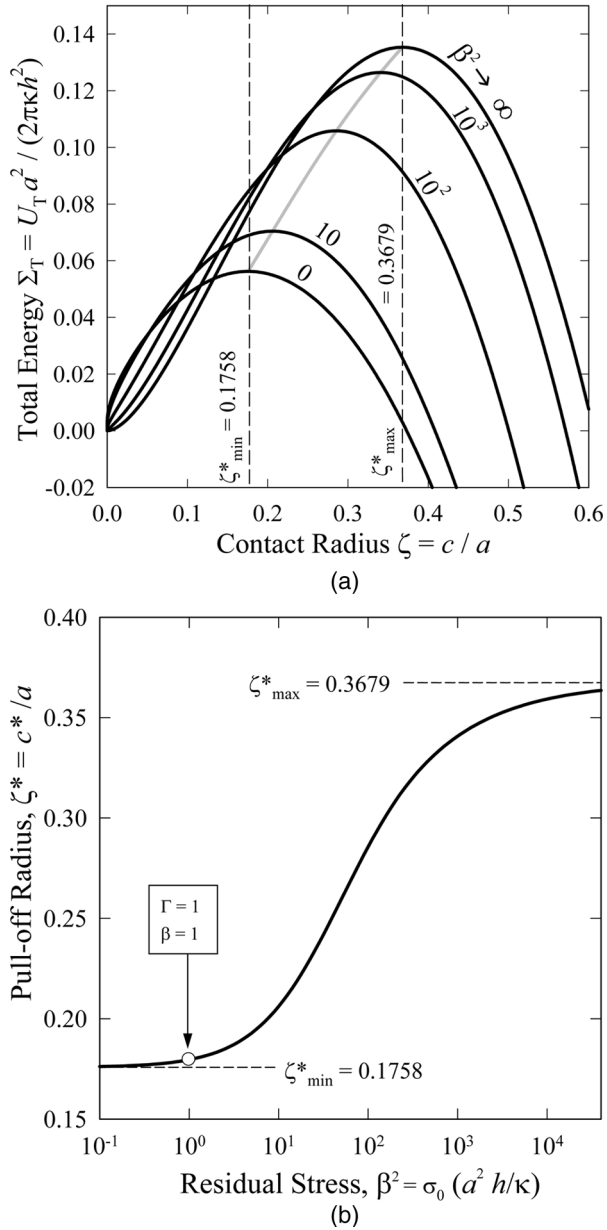

FIGURE 4 For a fixed adhesion energy ($\Gamma = 1$), the delamination trajectory is shown for a range of tensile residual stress. Pull-off occurs at the maximum of each curve. The gray curve joins the pull-off events. (b) Pull-off radius bounded by ζ^*_{min} and ζ^*_{max} is shown as a function of residual stress. The open symbol corresponds to $\Gamma = 1$ (*cf.* Figure 2).

thermodynamic equation (5). For an incremental shrinkage of the contact circle $(-\delta c), dU_T = d\Sigma_T = 0$, or $(\partial U_T/\partial c) = (\partial \Sigma_T/\partial \zeta) = 0$. Using Eq. (5), we get

$$\gamma = \frac{F}{2}\left[\frac{dw_0}{d(\pi c^2)}\right]_{F=\text{constant}} \quad \text{or} \quad \Gamma = \frac{\varphi}{2}\left[\frac{d\omega_0}{d(\zeta^2)}\right]_{\varphi=\text{constant}}. \tag{6}$$

Substituting Eq. (3) into Eq. (6), we get

$$\varphi = \left[2\beta\zeta\frac{I_1(\beta)K_1(\beta\zeta) - I_1(\beta\zeta)K_1(\beta)}{I_1(\beta)K_0(\beta\zeta) + I_0(\beta\zeta)K_1(\beta) - 1/\beta}\right]\Gamma^{1/2}. \tag{7}$$

Equation (7) requires both φ and ω_0 to be proportional to $\Gamma^{1/2}$ [because $\varphi \propto \omega_0$ in Eq. (3)], and Γ can be factored out from the right-hand side of Eq. (5). Because pull-off requires $(\partial \Sigma_T/\partial \zeta) = 0$, once β is fixed, ζ^* is automatically determined and is therefore independent of Γ.

To derive $\varphi(\omega_0)$ for the delamination process, ζ can be eliminated from Eq. (3) and Eq. (6). To circumvent the formidable mathematical operation, the exact form of $\varphi(\omega_0)$ can be found by a parametric method with a varying parameter ζ, because both φ and ω_0 are functions of ζ. Figure 5 shows $\varphi(\omega_0)$ with $\Gamma = 1.00,\ \beta = 1.00$ for a punch with radius $\zeta_A = 0.5702$. Delamination follows the trajectory OABCD (*cf.* curve ABC in Figure 2). Along the path OA, external loading results in a continuous deformation of the annulus (a–c) but does not cause delamination because of insufficient elastic energy stored in the annular film. The loading process is linear because of the linear $\varphi(\omega_0)$ according to Eq. (3). As the punch moves beyond point A, delamination starts to propagate according to Eq. (7). Further increase in ω_0 reduces the external load and shrinks the contact circle along ABC. Point C denotes the last point on the energy balance curve. Here the gradient of $\varphi(\omega_0)$ tends to infinity, *i.e.*, $(d\varphi/d\omega_0) \to \infty$. Further increase in ω_0 violates the energy balance. Pull-off occurs, and the external load drops to zero at D. The critical values of φ^*, $\omega_0{}^*$, and ζ^* at pull-off can be experimentally measured, yielding both the adhesion energy and residual stress. The nonphysical branch CO is a direct result of the mathematical energy balance only and is shown as the dashed curve in Figure 2. If the cylinder has exactly the same diameter as the clamped film, the overhanging annulus (a–c) vanishes and a theoretically infinite external load is required to initiate delamination. Such a force singularity is a direct consequence of the *membrane* deformation assumption. When the delaminated annulus has a width much smaller than the film

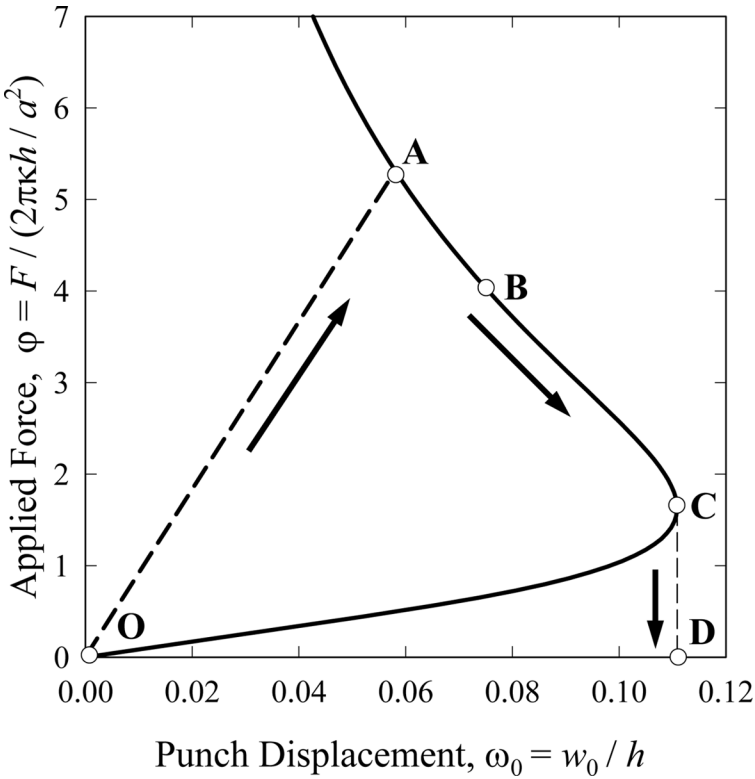

FIGURE 5 Mechanical response for $\Gamma = 1$ and $\beta^2 = 1$. The stable delamination trajectory follows OABC. Pull-off occurs at C. The branch CO is physically inaccessible.

thickness [*i.e.*, $(a–c) \ll h$] in the crack initiation stage, the mechanical stress is confined to a small region around the delamination front, the characteristics of being a film subjected to bending–stretching is lost, and Eq. (1) breaks down. In fact, the initiation load is *finite* in an ultrathin membrane with zero flexural rigidity [23]. The exact solution for the delamination initiation stage is beyond the scope of this article.

The coupling effects of adhesion and residual stress are demonstrated in Figures 6 and 7. Figure 6 shows the delamination path with $\beta = 1.00$ with a varying Γ. The curve labeled ABC is identical to that in Figure 2. The gray curve connects the pull-off events. Increasing adhesion energy shifts φ^* and $\omega_0{}^*$ to higher values, as expected.

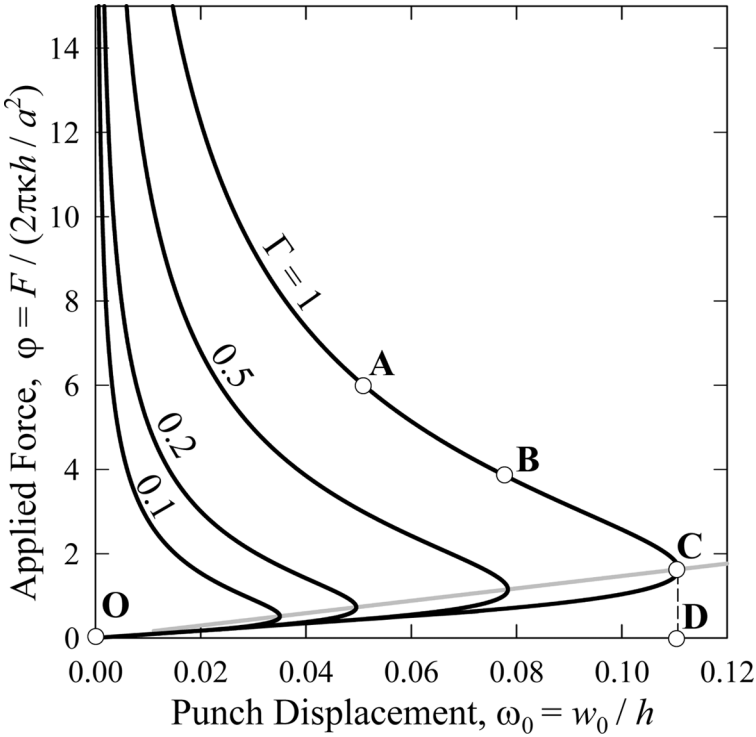

FIGURE 6 Delamination path for residual membrane stress $\beta^2 = 1$ and a range of adhesion energy. A stronger interfacial adhesion requires pull-off to occur at larger punch displacement. The gray line joins the pull-off events.

Because both φ and ω_0 are proportional to $\Gamma^{1/2}$ and ζ^* is a constant for fixed β [*cf.* (3) and (7)], it can be easily deduced that $\varphi^* \propto \omega_0^*$. Figure 7 shows the delamination path with $\Gamma = 1.00$ with a varying β. The gray curve connects all the pull-off events. The limiting case of $\beta \to \infty$ leads to two remarkable results, namely,

$$\varphi^* = \left(\frac{4}{e^2}\right)\frac{1}{\omega_0^*} \tag{8}$$

as derived from Eq. (3) and Eq. (6), and $\zeta^* = \zeta^*_{\max} = e^{-1}$. Increasing residual stress stiffens the film and shifts the pull-off event to a higher φ^* but a lower ${\omega_0}^*$.

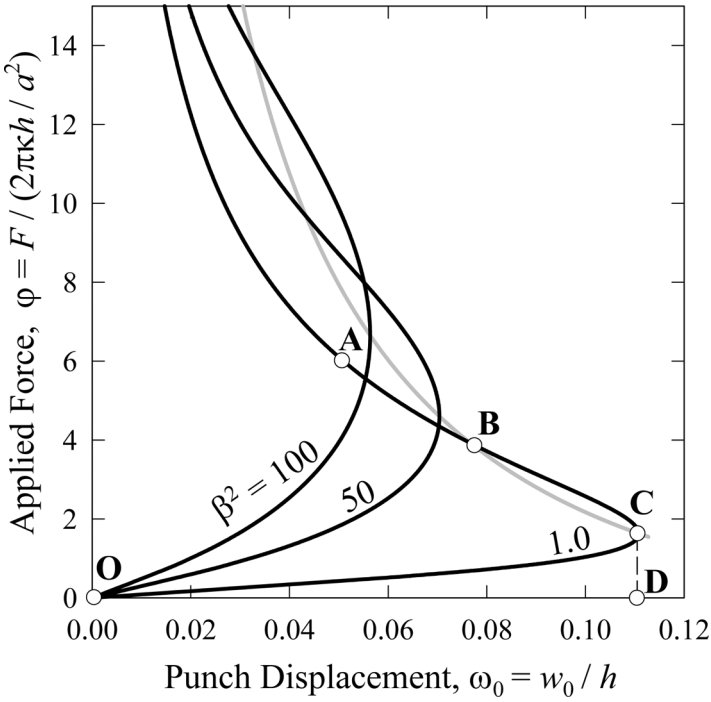

FIGURE 7 Delamination path for adhesion energy $\Gamma = 1$ and a range of residual membrane stress. Larger residual stress requires pull-off to occur at a smaller punch displacement and larger external load. The gray line joins the pull-off events.

3. DISCUSSION

A few remarks on the model assumptions and implications are warranted. Foremost, the deformed film profile upon external load could lead to a nonzero concomitant membrane stress in addition to the intrinsic residual stress. The error will be most significant at the bending–stretching transition when the total elastic energy U_{E} comprises comparable bending and stretching components. This occurs when the punch displacement is roughly the film thickness ($w_0 \approx h$). Nevertheless, the current work shows the transition from a bending-dominant mode to a stretching-dominant mode at an increasing residual membrane stress. In fact, the limiting case of an infinite residual stress coincides with the pure stretching model for thin membranes as shown in our earlier work [24]. In summary, according to Figure 4b, (i) when the residual stress falls below roughly $\beta_{\min} = 1$

or $(\sigma_0)_{\min} = (\kappa/a^2h)$, the film is governed by bending only and the effect of residual stress can be ignored; (ii) when the residual exceeds roughly $\beta_{\max} = 10^3$ or $(\sigma_0)_{\max} = 10^3\ (\kappa/a^2h)$, the bending component can be ignored; and (iii) in the intermediate range $(\beta_{\min} < \beta < \beta_{\max})$, the concomitant stress should be considered, though its inclusion leads to a slight shift in the mechanical response only.

Notwithstanding the main focus of this article on thin film delamination, the complementary adhesion mechanics is virtually equivalent, with some remarkable differences. If a microprobe is made of a clamped freestanding film to measure surface forces of a certain sample, the thermodynamic energy balance can be formulated in exactly the same manner as before, though the zero-range surface force assumed in the current model must be modified accordingly. When the probe moves to a distance $w_0{}^*$ from the sample surface, the film is energetically more favorable to jump into adhesive contact, or pull-in. In fact, pull-off and pull-in are equivalent in thermodynamic terms. However, a long-range interaction is required for pull-in to occur. If the surface force range is shorter than $w_0{}^*$, the film will stay largely undeformed because of an energy barrier across the gap. Conversely, a long-range force with range exceeding $w_0{}^*$ will trigger pull-in.

The current model can be easily transformed to discuss a one-dimensional equivalence, *i.e.*, a rectangular film clamped at either end as in a typical capacitive RF-MEMS switch [24]. Here a metallic bridge is mechanically suspended over an electrostatic pad. A critical electrical potential applied to the pad will compel the film to make contact with the substrate, thus grounding the circuit. As the switch dimension gets smaller, intersurface forces due to stray charges, intrinsic van der Waals interaction, and formation of meniscus due to water condensation become so significant that the film might remain in contact (or stiction) with the pad even at the removal of the applied potential, leading to disruption of normal device operation, if not permanent damage. The presence of residual stresses due to fabrication procedures and mismatch in thermal expansion coefficients during operation would further exacerbate the problem. Important parameters such as pull-in and pull-off film-pad separation, contact area, and the force–displacement relation provided in this article are essential in designing the optimal device geometry and dimensions and serve as indispensable guidelines in assessing device reliability.

Cell locomotion is a relevant example in biology. When a cell attempts to move in a certain direction, the actin filaments construct a makeshift pseudopodium that makes an adhesive contact or focal adhesion plaque with the substrate, similar to Figure 1. Retraction

of the hind "leg" then pulls the anchoring membrane out of contact, allowing the cell to move a step forward. The construction and destruction of the adhesive contacts can be discussed using our new model. If the intersurface forces are from ligand–receptor interaction, the adhesion mechanism also involves receptor diffusion in and out of the interface, as discussed in detail by Freund and Lin [25] using a model similar to the present work. They assume plate-bending of the cell wall in formation of focal adhesion plaque and ignore all membrane stretching, which could be the main deformation mode in many ultrathin biological membranes [25]. Residual membrane stress generated as a result of osmosis in the case of a differential gradient of liquid concentration within and without the cell [15] and viscoelasticity of cell membrane and network of actin filaments and extracellular matrix [26] further complicate the locomotion mechanics. The simple model here is not meant to be comprehensive in explaining these complex biological phenomena but, to provide a rigorous solid-mechanics basis for the underlying mechanical aspects. Correlation between mechanics and biochemistry is beyond the scope of this article.

4. CONCLUSION

A theoretical model is constructed for the adhesion–delamination mechanics of a circular film adhered to a rigid punch based on bending deformation of film subjected to tensile residual stress and a thermodynamic energy balance. The model relates (i) measurable quantities: applied load, punch displacement, and contact radius; (ii) deducible materials parameters: interfacial adhesion energy and residual stress; (iii) intrinsic materials parameters: elastic modulus and flexural rigidity of film; and (iv) geometrical dimensions: punch radius and film radius and thickness. The force–displacement relation and the pull-off reminiscent of the JKR model are derived and quantified in terms of the aforementioned quantities. The model provides a way to extract useful parameters from the measured data. The trends and graphs have significant impact on the design and fabrication of some MEMS involving moveable thin-film components and also cell adhesion and locomotion.

ACKNOWLEDGMENTS

This work was supported by National Science Foundation CMS (No. 0527912) and University of Missouri Research Board (No. 2428). M. F. W is partly supported by the Opportunities for Undergraduate

Research Experiences (OURE) program at University of Missouri–Rolla. The authors are grateful to Scott Julien for invaluable discussion and the many useful comments by the reviewers.

APPENDIX 1: DIRAC DELTA FUNCTION TO DENOTE EXTERNAL LOAD

The Dirac delta function $\delta(r)$ in the governing equation (1) needs further explanation. Within the contact ($r < c$), the film is planar, $w = w_0$, and therefore $dw/dr = 0$, implying zero mechanical force acting on the film. Without the contact ($r > c$), the noncontact overhanging part is not subject to any load. Therefore, the force must be a line force at the circular contact edge. Because the contact radius varies as delamination proceeds, it is mathematically correct to leave the source function as $F\delta(r)$. This can be easily proved by integrating Eq. (1) with respect to r, leading to

$$\kappa\left(\frac{d^3w}{dr^3}+\frac{1}{r}\frac{d^2w}{dr^2}-\frac{1}{r^2}\frac{dw}{dr}\right)-\sigma h\left(\frac{dw}{dr}\right)=\frac{F}{2\pi r}, \qquad \text{(A1-1)}$$

with the first bracket representing the shear force. The right-hand side is the line force at the contact edge with a length of $2\pi r$. An alternative interpretation of Eq. (1) is that the central point load applied to the punch $F\delta(r)$ is distributed to a line load at the contact edge ($r = c$). Provided the aforementioned boundary conditions are satisfied, the delta function will not lead to a singularity. Equation (A1-1) is mathematically equivalent to Eq. (1).

APPENDIX 2: NORMALIZED PARAMETERS

For simplicity, the geometrical parameters are cast as follows:

$$\omega=\frac{w}{h}, \qquad \omega_0=\frac{w_0}{h}, \qquad \xi=\frac{r}{a}, \qquad \zeta=\frac{c}{a} \qquad \text{(A2-1)}$$

with the vertical deflection of the film normalized by the film thickness, and the radial distances normalized by the film radius. Rewriting Eq. (1) using these dimensionless variables, the mechanical force consequently becomes

$$\varphi=\frac{Fa^2}{2\pi\kappa h} \qquad \text{(A2-2)}$$

When we substituting Eqs. (A2-1) and (A2-2) into Eqs. (4) and (5), the energy terms, interfacial adhesion energy, and tensile residual stress are normalized as

$$\Sigma = \frac{a^2}{2\pi\kappa h^2}U, \qquad \Gamma = \left(\frac{a^4}{2\kappa h^2}\right)\gamma, \qquad \beta = \left(\frac{a^2 h}{\kappa}\right)^{1/2}\sigma_0^{1/2} \qquad \text{(A2-3)}$$

respectively. Note that β is the ratio of the tensile membrane stress (σ_0) to the bending inertia (κ). Film deformation is therefore dominated by plate bending for $\beta \to 0$ and by membrane stretching for $\beta \to \infty$.

REFERENCES

[1] Xu, T.-B. and Su, J., *Sensors and Actuators A* **121**, 267–274 (2005).
[2] Prochaska, A. M., Nemirovsky, Y., and Dinnar, U., *Journal of Micromechanics and Microengineering* **15**, 2309–2316 (2005).
[3] Ullmann, A., Fono, I., and Taitel, Y., *Journal of Fluids Engineering* **123**, 92–98 (2001).
[4] Oh, K. W. and Chong, H. A., *Journal of Micromechanics and Microengineering* **16**, R13–R39 (2006).
[5] Najar, F., Choura, S., El-Borgi, S., Adbdel-Rahman, E., and Nayfeh, A., *Journal of Micromechanics and Microengineering* **15**, 419–429 (2005).
[6] Vogl, G. and Nayfeh, A., *Journal of Micromechanics and Microengineering* **15**, 684–690 (2005).
[7] Elders, J., Spiering, V., and Walsh, S., *Microelectromechanical Systems: Technology and Applications* **26**, 312–317 (2001).
[8] Rebeiz, G. M. and Muldavin, J. B., *IEEE Microwave Magazine* **2**, 59–71 (2001).
[9] Osterberg, P. and Senturia, S., *Journal of Microelectromechanical Systems* **6**, 107–118 (1997).
[10] Nemirovsky, Y., *Journal of Microelectromechanical Systems* **10**, 601–615 (2001).
[11] Chowdhury, S., Ahmadi, M., and Miller, W., *Journal of Micromechanics and Microengineering* **15**, 756–763 (2005).
[12] Evans, D. F. and Wennerstrom, H., *The Colloidal Domain: Where Physics, Chemistry, and Biology Meet* (Wiley, New York, 1999).
[13] Israelachvili, J. N., *Intermolecular and Surface Forces*, 2nd ed. (Academic Press, London, 1991).
[14] Alberts, B., Bray, D., Lewis, J., Raff, M., Roberts, K., and Watson, J. D., *Molecular Biology of the Cell* (Garland, New York, 1994).
[15] Wan, K.-T. and Liu, K. K., *Medical and Biological Engineering and Computing* **39**, 605–608 (2001).
[16] Liu, K. K., Wang, H. G., Wan, K.-T., Liu, T., and Zhang, Z., *Colloids and Surfaces B: Biointerfaces* **25**, 293–298 (2002).
[17] Foo, J. J., Chan, V., and Liu, K. K., *Annals of Biomedical Engineering* **31**, 1279–1286 (2003).
[18] Foo, J. J., Liu, K. K., and Chan, V., *AICHE* **50**, 249–254 (2004).
[19] Kendall, K., *Molecular Adhesion and Its Application: The Sticky Universe* (Kluwer Academic/Plenum Publishers, New York, 2001).
[20] Maugis, D., *Contact, Adhesion and Rupture of Elastic Solids* (Springer, New York, 2000).
[21] Wan, K.-T., *Journal of Applied Mechanics* **69**, 110–116 (2002).
[22] Wan, K.-T. and Dillard, D. A., *Journal of Adhesion* **79**, 123–140 (2003).

[23] Raegen, A. N., Dalnoki-Veress, K., Wan, K.-T., and Jones, R. A. L., *The European Physical Journal E* **19**, 453–459 (2006).
[24] Wan, K.-T. and Kogut, L., *Journal of Micromechanics and Microengineering* **15**, 778–784 (2005).
[25] Freund, L. B. and Lin, Y., *Journal of the Mechanics and Physics of Solids* **52**, 2455–2472 (2004).
[26] Boal, D., *Mechanics of the Cells* (Cambridge University Press, New York, 2002).